Purdue University
Purdue e-Pubs

International Refrigeration and Air Conditioning Conference

School of Mechanical Engineering

2008

Effect of Void Fraction Model on the Dynamic Performance of Moving Boundary Heat Exchanger

Omar Abdelaziz
University of Maryland

Vikrant Aute
University of Maryland

Reinhard Radermacher
University of Maryland

Follow this and additional works at: http://docs.lib.purdue.edu/iracc

Abdelaziz, Omar; Aute, Vikrant; and Radermacher, Reinhard, "Effect of Void Fraction Model on the Dynamic Performance of Moving Boundary Heat Exchanger" (2008). *International Refrigeration and Air Conditioning Conference.* Paper 991.
http://docs.lib.purdue.edu/iracc/991

This document has been made available through Purdue e-Pubs, a service of the Purdue University Libraries. Please contact epubs@purdue.edu for additional information.
Complete proceedings may be acquired in print and on CD-ROM directly from the Ray W. Herrick Laboratories at https://engineering.purdue.edu/Herrick/Events/orderlit.html

Effect of Void Fraction Model on the Dynamic Performance of Moving Boundary Heat Exchanger

Omar AbdelAziz[1]*, Vikrant Aute[2], Reinhard Radermacher[3]

Center for Environmental Energy Engineering
Department of Mechanical Engineering, University of Maryland
College Park, MD 20742 USA
[1] Tel: 301-405-8726, Fax: 301-405-2025, Email: oabdelaz@umd.edu
[2] Tel: 301-405-8726, Email: vikrant@umd.edu
[3] Tel: 301-405-5286, Email: raderm@umd.edu

*Indicate Corresponding Author

ABSTRACT

Transient simulation of refrigeration systems is a relevant tool in the development and optimization of household refrigerators. These models should be accurate but fast. The core of transient refrigeration system simulation is the heat exchanger model as it imposes the system pressures. Dynamic pressure variation inside the heat exchanger is governed by the apparent density and internal energy of the refrigerant. For two-phase flow, the void fraction determines the apparent density. Several void fraction models are available in literature; each model provides different values of void fraction for the same refrigerant conditions. Unfortunately, a 1% error in void fraction could lead to 16% error in apparent density at a void fraction of 95%. In the current study a moving boundary heat exchanger model was developed to simulate the dynamic performance during pull-down in a typical four component vapor compression system. In this model, the void fraction can be calculated based on 12 different void fraction models. A parametric study is performed on the effect of void fraction models on the performance of small refrigeration systems using a system simulation software. System pressures and charge distribution were compared for the different void fraction model.

1. INTRODUCTION

The need for higher efficiency household refrigerators created the need for reliable, accurate and efficient transient refrigeration system simulation in order to cut back on the research and development cost and time. Improving model reliability and accuracy comes at the cost of increased modeling details and increased computational cost. Therefore, a tradeoff between model accuracy and computational cost should always be considered while developing new simulation tools. Previous dynamic vapor compression simulations: Anand (1999), (Bendapudi *et al.* 2002) incorporated bulk entity transient heat exchanger models (Jacobsen, 1995); further investigation by Willatzen *et al.* (1998) and Pettit *et al.* (1998) gives a complete formulation of two phase flow heat exchangers which includes a lumped three region transient model. A new concept for phase segment assignment based on the charge distribution was used in Abdelaziz *et al.* (2006) based on the Lokhart-Martinelli void fraction model. The operating range of household refrigerator evaporators has not been thoroughly investigated before, especially for void fraction and heat transfer correlations. The evaporator mass flux is usually between 15 and 70 kg/m^{2}s, which are on the lower limit or below the range of validity for most of the available correlations. This paper investigates the difference in numerical results, just by changing void fraction model for the same system configuration. The proposed heat exchanger(HX) model is composed of three segments of variable lengths to account for the development of the phase change locations. The performance of such heat exchanger model is governed by the refrigerant charge, bulk refrigerant state as well as inlet and outlet refrigerant states and mass flow rates. Numerical results shown at the end of this paper provide an insight into the effect of void fraction on the system simulation accuracy; however they do not provide the validity of void fraction models used under given configuration as these

are highly dependent on the heat exchanger design. Future validation studies are required to compare the model and suggest the void fraction model that provides the highest accuracy.

2. VOID FRACTION MODELS REVIEW

Rice (1987) investigated the effect of ten void fraction correlations and four heat flux assumptions on refrigerant charge inventory predictions in large air conditioning systems. The study showed that the choice of void fraction model has a major effect on refrigerant charge modeling. Reported results showed a maximum variation of predictions of a factor of 10 for low-ambient heating-mode evaporators. Farzad and O'Neal (1994) studied the effect of void fraction model on system performance. Eight void fraction models (Homogeneous, Lockhart and Martinelli, Thom, Zivi, Baroczy, Hughmark, Premoli and Tandon) were used in the model in the prediction of power, capacity, refrigerant flow, subcooling and superheat. The predictions were compared against a 10.6 kW capacity air conditioner with capillary tube expansion. The following subsections provide a review of the void fraction models used in the current work.

2.1 Void Fraction Correlations

Most of the void fraction correlations take the form shown in Equation (1). The coefficients listed in this Equation "B_B, n_1, n_2, n_3" have different values for different correlations as shown in Table 1. Carey (1992) and Thome (2004) provide a comprehensive review of void fraction models, the following is a description of the void fraction models considered in the present work; namely: Barcozy, Harms, Homogeneous, Hughmark, Lokhart Martinelli, Premoli, Rigot, Rouhani Axelsson, Smith, Tandon, Thom, and Zivi.

$$\alpha = \left[1 + B_B x_r^{n1} \rho_r^{-n2} \mu_r^{n3}\right]^{-1} \tag{1}$$

Table 1: Void faction model parameters for Equation (1) – Carey (1992)

Correlation or model	B_B	n_1	n_2	n_3
Homogeneous	1	1	1	0
Zivi	1	1	0.67	0
Wallis	1	0.72	0.4	0.08
Lokhart Martinelli	0.28	0.64	0.36	0.07
Thom	1	1	0.89	0.18
Barcozy	1	0.74	0.65	0.13

The homogenous void fraction model assumes both liquid and vapor travel inside the flow area at the same velocity. Hence, the void fraction can be derived from the continuity Equation. This model usually overestimates the void fraction and thus underestimates the system charge. Rigot, Smith, Zivi and Premoli void fraction models all fall under the slip-ratio correlated void fraction model category. The general form of the slip-ratio correlated models is shown in Equation (2). Rigot's model suggest the use of a slip ratio of 2.0 while the Smith model incorporates an Equation for the slip ratio based on equal momentum fluxes in the vapor and liquid flows due to droplets entrainment in the vapor region of a homogeneous mixture in the center and an annular liquid phase. The slip ratio correlation used in Smith void fraction model is given in Equation (3) where $K = 0.4$.

$$\alpha = \left[1 + x_r \rho_r^{-1} S\right]^{-1} \tag{2}$$

$$S = K + (1 - K)\left[\frac{\rho_r + K x_r}{1 + K x_r}\right]^{0.5} \tag{3}$$

Zivi void fraction correlation is based on principles of minimum entropy production under conditions of zero wall friction and zero liquid entrainment for an annular flow configuration. The slip ratio in Zivi's model is calculated using Equation (4). Premoli's correlation was optimized for liquid density prediction error, thus can be more accurate in the prediction of apparent two-phase refrigerant density. The slip ratio in Premoli's correlation is calculated based on Equation (5).

$$S = (\rho_r)^{1/3} \tag{4}$$

$$S = 1 + a\,\mathrm{Re}_L^{-0.19}\left(\rho_r\right)^{0.22}\left[\frac{y}{1 + byWe_L\,\mathrm{Re}_L^{-0.53}\left(\rho_r\right)^{-0.08}} - byWe_L\,\mathrm{Re}_L^{-0.53}\left(\rho_r\right)^{-0.08}\right]^{0.5} \tag{5}$$

Where:

$$\mathrm{a} = 1.578, \quad b = 0.0273, \quad y = \frac{\beta}{1-\beta}, \quad We_L = \frac{G^2 D}{\sigma \rho_f g}$$

Another void fraction model category is the X_{tt} Correlated model where the Lockhart- Martinelli correlating parameter X_{tt}, defined in Equation (6), is used to calculate the void fraction. The original Lockhart- Martinelli void fraction correlation takes the form shown is Equation (7). A modification to this model was assumed by Wallis for the $X_{tt} \leq 10$ as shown in Equation (8) and by Domanski and Didion for $X_{tt} > 10$ as show in Equation (9). Baroczy's void fraction correlation added a direct functional dependence on fluid properties beyond that already included in X_{tt}.

$$X_{tt} = x_r^{\,0.9}\mu_r^{\,0.1}\rho_r^{\,-0.5} \tag{6}$$

$$\alpha = \left(1 + 0.28X_{tt}^{0.71}\right)^{-1} \tag{7}$$

$$\alpha = \left(1 + X_{tt}^{0.8}\right)^{-0.378} \qquad \text{for } X_{tt} \leq 10 \tag{8}$$

$$\alpha = 0.823 - 0.157\ln X_{tt} \qquad \text{for } X_{tt} > 10 \tag{9}$$

Mass-Flux-Dependent void fraction models such as Tandon and Hughmark correlations incorporate the effect of wall friction based on either physical model (Tandon) or empirical data (Hughmark). Tandon's correlation account for mass flux by incorporating the Reynolds number (Re) as shown Equation (10). While Hughmark's correlation uses a correction factor to the homogenous model as shown in Equation (11). The correction factor is given in a tabulated form in Table 2 as a function of Z calculated based on Equation (12).

$$\alpha = \left[1 - \frac{1.928\,\mathrm{Re}_L^{-0.315}}{F\left(X_{tt}\right)} + \frac{0.9293\,\mathrm{Re}_L^{-0.63}}{F\left(X_{tt}\right)^2}\right], \text{ for } 50 < \mathrm{Re}_L < 1125,$$

$$\alpha = \left[1 - \frac{0.38\,\mathrm{Re}_L^{-0.088}}{F\left(X_{tt}\right)} + \frac{0.0361\,\mathrm{Re}_L^{-0.176}}{F\left(X_{tt}\right)^2}\right], \text{ for } \mathrm{Re}_L > 1125, \tag{10}$$

Where:

$$F\left(X_{tt}\right) = 0.15\left(\frac{1}{X_{tt}} + \frac{2.85}{X_{tt}^{\,0.476}}\right), \mathrm{Re}_L = \frac{GD\left(1-x\right)}{\mu_f}$$

$$\alpha = K_H \beta \tag{11}$$

$$Z = \left[\frac{DG}{\mu_f + \alpha\left(\mu_g - \mu_f\right)}\right]^{1/6}\left[\frac{1}{gD}\left(\frac{Gx}{\rho_g \beta\left(1-\beta\right)}\right)^2\right]^{1/8} \tag{12}$$

Table 2: Hughmark Correlation Correction Factor

Z	1.3	1.5	2.0	3.0	4.0	5.0	6.0	8.0	10.0	15.0	20.0	40.0	70.0	130.0
K_H	0.185	0.225	0.325	0.49	0.605	0.675	0.72	0.767	0.78	0.808	0.83	0.88	0.93	0.98

Finally, a drift flux void fraction model is used to incorporate the effect of relative volumetric flow rate of liquid and vapor with respect to a moving reference frame at the mean velocity. The average value for the void fraction over a given tube segment is given by Equation (13).

$$\alpha = \frac{x}{\rho_g}\left[C_0\left(\frac{x}{\rho_g} + \frac{1-x}{\rho_l}\right) + \frac{\overline{U}_{GU}}{\dot{m}}\right]^{-1} \tag{13}$$

Rouhani-Axelsson correlated the void fraction in vertical channels using the drift-flux model, the correlation parameters C_0 and $\overline{U}_{GU}$ can be calculated as shown in Equations (14) and (15) respectively.

$$C_0 = 1 + 0.2(1-x)\left(\frac{g d_i \rho_l^2}{\dot{m}^2}\right) \quad (14) \qquad \overline{U}_{GU} = 1.18\left[\frac{g\sigma(\rho_l - \rho_g)}{\rho_l^2}\right]^{1/4} \quad (15)$$

For horizontal channel, a modified version of Rouhani-Axelsson, Steiner correlation, is used. The drift-flux parameters C_0 and $\overline{U}_{GU}$ are calculated based on Equations (16) and (17) respectively.

$$C_0 = 1 + 0.12(1-x) \quad (16) \qquad \overline{U}_{GU} = 1.18(1-x)\left[\frac{g\sigma(\rho_l - \rho_g)}{\rho_l^2}\right]^{1/4} \quad (17)$$

2.2 Void Fraction Model Validation

Wojtan (2004) used a new optical void fraction measurement technique to experimentally determine the void fraction of R22 and R410A at different mass fluxes, saturation pressures and qualities. The experimental database was used to validate 4 different void fraction correlations namely: homogeneous, Zivi, Taitel-Dukler and Rouhani-Axelsson. The reported relative error and standard deviation were grouped by the mass flux. The validation results show that homogeneous model has the highest relative error while Taitel-Dukler is the best for pure refrigerants and Rouhani-Axelsson is better for refrigerant mixtures. Based on the validation results, homogeneous void fraction model represents the upper bound for the void fraction value.

3. TRANSIENT MOVING BOUNDARY HEAT EXCHANGER MODEL

The transient moving boundary heat exchanger model described in this work is an enhancement to the model proposed in Abdelaziz et al. (2006). The model incorporates moving boundaries to model the vapor, two-phase and liquid zones separately. Figure 1 below illustrates the heat exchanger with the two moving boundary limits. Control volumes I, II, III are for the refrigerant, wall, and air respectively. Unlike previous transient heat exchanger models, the two-phase region void fraction is calculated based on the different void fraction models described in section 2 above. This model is used to simulate both heat exchangers (condenser and evaporator) in a transient system simulation tool as described in the work of Anand (1999), Gercek *et al*. (2005) and Abdelaziz *et al*., (2006).

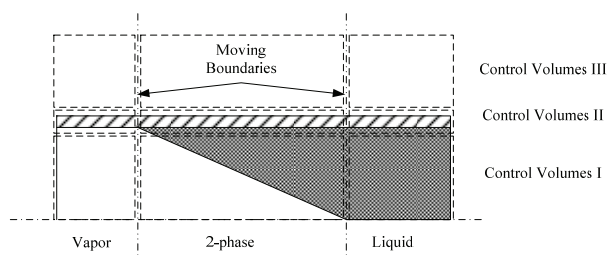

Figure 1: Heat exchanger refrigerant model description

3.1 Model Assumptions

The actual governing Equations (transient 3D Navier-Stokes and Energy Equations) can not be solved analytically while numerical solution would require huge computational resources. In order to reduce the problem, some assumptions are made such that the model can be solved as part of a transient refrigeration system simulation. These assumptions are: one dimensional inviscid fluid flow, equal inlet and outlet mass flow rates in the single phase regions, constant heat transfer coefficients between the refrigerant and the wall for each of the three regions, constant airside heat transfer coefficient, uniform wall temperature, equal mass and heat transfer fin effectiveness and Lewis number used for moist air is 1.0. It is further assumed that system mass flow rates are governed only by performance of the compressor and the orifice. Before iterating, the heat exchanger models' inlet and outlet mass flow rates and inlet enthalpy are updated. Pressure, charge and wall temperature are maintained by the component model and updated only before each time step. The model calculates outlet refrigerant state and total airside and refrigerant side heat transfer. In addition, wall temperature, internal energy and refrigerant charge gradients are evaluated for the time step updates.

3.2 Refrigerant Control Volume

The heat exchanger boundaries are determined based on a modified inlet refrigerant state and the refrigerant charge inside the heat exchanger. The modified inlet refrigerant state is based on the assumption that the heat transfer on the refrigerant side is based on the bulk refrigerant state. This assumption hold true since the time step is quit small and the time required for the inlet state to propagate through the heat exchanger length is an order of magnitude larger than the time step used in the transient simulation. The modified inlet state's internal energy is based on adiabatic mixing as shown in Equation (18), the modified inlet enthalpy is then estimated based on Equation (19). The charge limits are calculated based on Equations in Table 3. The average void fraction used in the two-phase refrigerant charge limit is averaged as shown in Equation (20) with the saturated properties evaluated at the current time step's heat exchanger pressure. Equation (20) is a function of the void fraction model of choice.

$$\left[\left(\dot{m}_{in}-\dot{m}_{out}\right)\Delta\tau+M\right]\widetilde{u_{in}}=\dot{m}_{in}\,\Delta\tau h_{in}+Mu_{avg}-\dot{m}_{out}\,\Delta\tau h_{out} \tag{18}$$

$$\widetilde{h_{in}}=\widetilde{u_{in}}+P\frac{V}{M} \tag{19}$$

Table 3: Heat Exchanger Charge Limits.

Charge limit	Symbol	Definition
Ideal 2-phase Charge (from x =0.0 to x = 1.0)	M_{fg}	$M_{fg}=\rho_{fg}\times V$, Where $\rho_{fg}=\alpha\times\rho_g+(1-\alpha)\times\rho_f$
All vapor	M_g	$M_g=\rho_g\times V$
all liquid	M_f	$M_f=\rho_f\times V$

$$\alpha_{x_{in}\to x_{out}}=\frac{\sum_{i=0}^{100}\alpha\left(P_{sat},x=0.01\times i\times\left(x_{in}-x_{out}\right)\right)}{101} \tag{20}$$

The HX type is determined based on the difference between the modified inlet temperature and wall temperature. If the wall temperature is less than the modified inlet temperature the heat exchanger cools the refrigerant, otherwise the heat exchanger heats the refrigerant. Based on the application type, the HX charge is compared with the limits calculated in Table 3 to determine the possible number of phases within the heat exchanger. Truth Tables 4 and 5 are used to determine the number of refrigerant phases for condensing and evaporating application respectively.

Table 4: Truth table for heat exchanger as condenser

Inlet Condition Check	Charge Limit Check	Configuration	Segments Assignment
$T_{in}<T_{sat}$	$M\geq M_f$	All liquid	$L_{liq}=L$; T_{out} based on H.T.
$0.0\leq x_{in}\leq 1.0$	$M>M_{gf}$	2-phase and liquid	charge balance in condensing/liquid region
	$M_g<M\leq M_{gf}$	only 2phase	$L_{2ph}=L$; outlet conditions based on charge balance
$T_{in}>T_{sat}$	$M<M_g$	Only Vapor	$L_{vap}=L$; T_{out} based on H.T.
	$M_g\leq M<M_f$	Up to 3 zones	L_{vap} = length required to reach T_{sat} $L_{2ph/liq}=L-L_{vap}$; charge balance in 2Ph/liq. region

Table 5: Truth table for heat exchanger as evaporator

Inlet Condition Check	Charge Limit Check	Configuration	Segments Assignment
$T_{in}>T_{sat}$	$M\leq M_g$	All vapor	$L_{vao}=L$; T_{out} based on H.T.
$0.0\leq x_{in}\leq 1.0$	$M<M_{gf}$	2-phase and vapor	charge balance in evaporating/vapor region
	$M_{gf}\leq M<M_f$	Only 2phase	$L_{2ph}=L$; outlet conditions based on charge balance
$T_{in}<T_{sat}$	$M\geq M_f$	Only liquid	$L_{liq}=L$; T_{out} based on H.T.
	$M_g\leq M<M_f$	Up to 3 zones	L_{liq} = length required to T_{sat} $L_{2ph/vap}=L-L_{liq}$; charge balance in 2Ph/Vap. region

For the most general case, with a single phase inlet, two phase region and a single phase outlet; the first single phase segment's length is calculated based on the heat transfer area required for the outlet to reach the saturation temperature. The remainder length of the heat exchanger is divided between the two-phase and single phase according to charge distribution. For condensing application, Equations (21), (22), and (23) are solved simultaneously to determine the length of each segment and the refrigerant outlet conditions. These Equations represent the geometry constraints, charge conservation and heat transfer in the liquid region respectively.

$$L_{2ph,liq} = L_{2ph} + L_{liq} \tag{21}$$

$$M_{2ph,liq} = L_{2ph}\rho_{xin\to 0.0} + L_{liq}\left(\frac{\rho_f + \rho_{out}}{2}\right) \tag{22}$$

$$\dot{m}_{out}\, Cp_{liq,avg}\left(T_{sat} - T_{out}\right) = U_{liq}\left(\pi D_{in} L_{liq}\right)\frac{\left(T_{sat} - T_{out}\right)}{\ln\left(\frac{\left(T_{sat} - T_{wall}\right)}{\left(T_{out} - T_{wall}\right)}\right)} \tag{23}$$

3.3 Wall Control Volume

The energy balance in the wall control volume is used to determine the wall temperature derivative as shown in Equation (24) assuming a sign convention such that the refrigerant heat transfer is from the refrigerant to the wall and the air side heat transfer is from the wall to the air. The overall H.X. wall temperature derivative used to update the wall temperature between time steps is a length based average of all three segments.

$$MC_{wall}\frac{dT_{wall}}{d\tau} = Q_{ref} - Q_{air} \tag{24}$$

3.4 Air Control Volume

For the airside control volume, the air thermal mass is neglected and cross flow configuration is used to simulate the sensible and latent heat transfer to the moist air. The enthalpy potential method described in McQuiston *et al.* (2005) is used to estimate the airside heat transfer for each segment. The airside sensible heat transfer is calculated as in Equation (25) based on the assumptions described in section 3.1. The airside mass flow rate for each segment is weighted based on its length. The effective airside area takes into account the fin ratio and the fin efficiency.

$$Q_{sensible} = \dot{m}_{air}\, Cp_{air}\left(T_{air,in} - T_{air,out}\right) = U_{air}\left(A_{air,effective}\right)\frac{\left(T_{air,in} - T_{air,out}\right)}{\ln\left(\frac{\left(T_{air,in} - T_{wall}\right)}{\left(T_{air,out} - T_{wall}\right)}\right)} \tag{25}$$

The total airside heat transfer is calculated based on the mass transfer coefficient (U_D), saturated air enthalpy at the wall temperature and the inlet air enthalpy as shown in Equation (26) below.

$$Q_{total} = U_D A_{air,effective}\left(h_{air,in} - h_{saturated\ air,wall}\right) \tag{26}$$

Hence, the latent heat transfer is simply the difference between the total and sensible load, and the outlet humidity ratio can be calculated as in Equation (27).

$$\psi_{out} = \psi_{in} - \frac{Q_{total} - Q_{sensible}}{\dot{m}_{air}\, h_{fg,water}} \tag{27}$$

To calculate the overall outlet air conditions from the three segments of the heat exchanger, adiabatic mixing between the outlet air streams of the three segments is performed.

4. NUMERICAL RESULTS

In order to test the different void fraction models, the aforementioned model is used for the simulation of both the evaporator and condenser in TransRef (Abdelaziz *et al.* (2006)). The evaporator is a 9.86m long, 5.7 mm diameter tube with 0.03 kg/s of air flow across it. The condenser is a 3.92 m long, 6.5 mm diameter tube with 0.1 kg/s of air flow across it. The compressor has a displacement of 7 cm^3 and runs at 3600 RPM while the orifice diameter is 0.4

mm. The evaporator is coupled with a typical single display cabinet freezer. The whole system starts from equilibrium conditions at 298.15 K and runs for 12000 s of simulation time. Twelve void fraction models were used for this system simulation to determine the effect of selected void fraction model on the results.
Of the 12 tested models, 5 have failed due to fast depletion of evaporator charge in the first 20 seconds. The models which failed to simulate the system under consideration are: Homogeneous, Zivi, Smith, Thom and Rigot. In these models, the overestimated void fraction allowed for a dominated condensation segment in the condenser which led to slower increase in condenser pressure which affected the performance of the orifice and led to evaporator starvation.

The condensing and evaporating pressures for the other 7 models (Lokhart-Martinelli, Barcozy, Harms, Hughmark, Permoli, Rouhani-Axelsson and Tandon) are plotted against simulation time in Figures 2 and 3 respectively. Finally, comparisons of the condenser and evaporator charges with different models are shown in Figures 4 and 5.

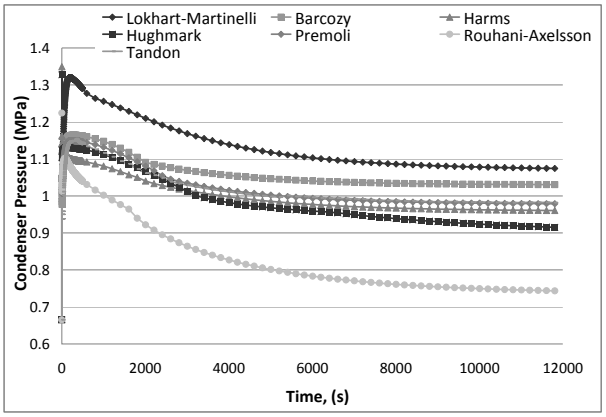

Figure 2: Condensing pressure during pull-down

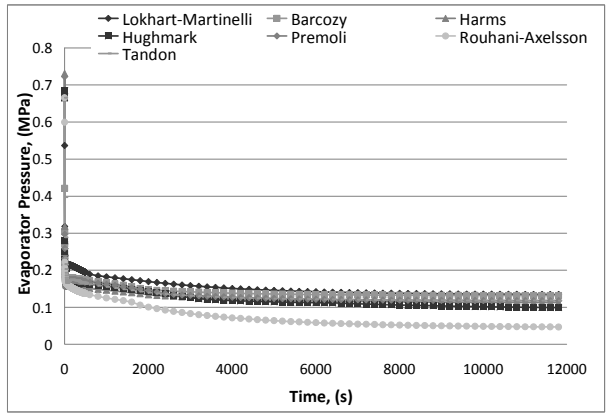

Figure 3: Evaporating pressure during pull-down

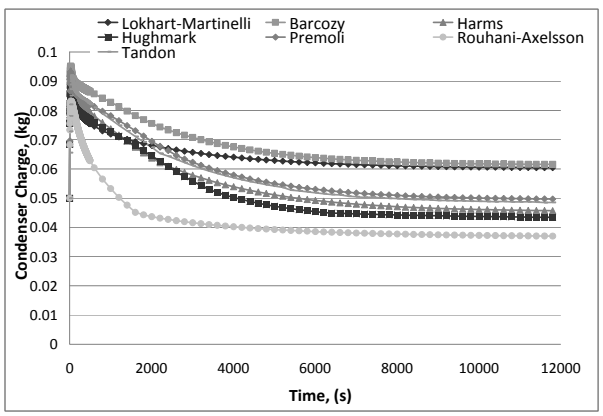

Figure 4: Condenser charge during pull-down

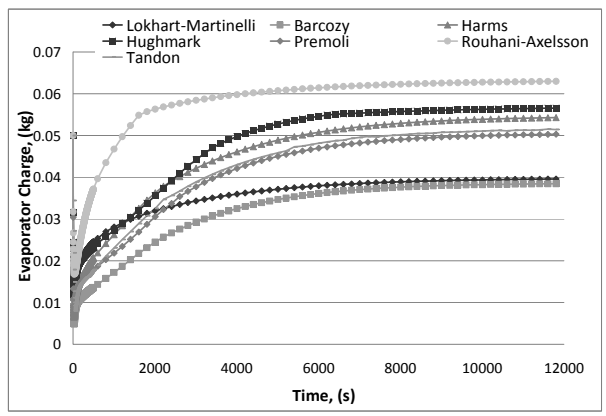

Figure 5: Evaporator charge during pull-down

5. CONCLUSIONS

The performance of a transient refrigerator simulation model versus different void-fraction calculation methods has been investigated. Results show that Barcozy, Harms, Hughmark, Lokhart-Martinelli, Premoli, Rouhani-Axelsson, and Tandon correlations follow the same trend except for Rouhani-Axelsson model. The system charge distribution for Lokhart-Martinelli and Barcozy models are different in the first 6000 s but reach the same asymptotic values at 12000 s. The difference during initial pull-down is due to the large condenser pressure gradient in the Lokhart-Martinelli case. Excluding the Rouhani-Axelsson model, the average for the system capacity at 12000 s is 67.66 W with a standard deviation of 9% for the evaporator and 338 W with a standard deviation of 15% for the condenser. The acceptable standard deviation in these results suggests that the use of any of the 6 models would be appropriate for the transient simulation of refrigeration cycles.

NOMENCLATURE

c_p	specific heat	(J/kg.K)	μ	Dynamic Viscosity	(Pa.s)
D	internal tube diameter	(m)	ρ	Density	(kg/m^3)
G	mass flux	(kg/m^{2}s)	ρ_r	ρ_f / ρ_g	(–)
h	enthalpy	(J/kg)	τ	Time	(s)
L	length	(m)		**Subscript**	
$\dot{m}$	mass flow rate	(kg/s)	2ph	two phase	
M	charge	(kg)	f	saturated liquid	
P	refrigerant pressure	(Pa)	fg	2-phase	
T	temperature	(K)	g	saturated vapor	
U	average heat transfer Coefficient	(W/m^2.K)	$H.X.$	heat exchanger	
V	heat exchanger internal volume	(m^3)	in	inlet	
x	vapor quality	(–)	liq	liquid	
x_r	$(1-x)/x$	(–)	out	outlet	
α	Void fraction	(–)	ref	refrigerant	
β	$[1+x_r\rho_r]^{-1}$	(–)	sat	saturation	
μ_r	μ_f / μ_g	(–)	vap	vapor	

REFERENCES

Abdelaziz, O., Winkler, Aute, V., Radermacher, R, 2006, Transient Simulation of a Transcritical Carbon Dioxide Refrigeration System, *11th Int. Ref. and A-C Conf. at Purdue*, R93

Anand, G., 1999, Transient and steady state model of a household refrigerator, *M. Sc. Thesis*, University of Maryland College Park, MD, USA.

ASHRAE, 2005, *ASHRAE Handbook of fundamentals (SI Edition)*, ASHRAE, GA, USA p.

Bendapudi, S., Braun, J., Groll, E., 2002, A Dynamic Model of a Vapor Compression Liquid Chiller, *9th Int. Ref. and A-C Conf. at Purdue*, R9-2

Carey, V.P., 1992, *Liquid – Vapor phase change phenomena, an introduction to the thermophysics of vaporization and condensation processes in heat transfer equipment*, Series in Chemical and Mechanical Engineering, Taylor and Francis, Hemisphere publishing corporation, USA, p. 432-433.

Farzad, M., O'Neal, D. L., 1994, "The Effect of Void Fraction model on estimation of air conditioner system performance variables under a range of refrigerant charging conditions", International Journal of Refrigeration, 1994, Vol. 17 No. 2, p. 85-93

Gercek E., Aute V., Radermacher R., 2005, Transient Simulation Tool for Refrigeration Systems, *IIR Conf. on Comm. Ref., Vicenza, Italy*, August 2005.

Lemmon, E.W., McLinden, M.O., Huber, M.L., 2002, REFPROP 7.0. Thermodynamic and transport properties of refrigerants and refrigerant mixtures. *NIST*, Gaithersburg, MD, USA.

McQuiston, F.C., Parker, J.D., Spitler, J.D., 2005, *Heating, Ventilating and Air Conditioning: Analysis and Design*, 6th Edition, John Wiley and Sons Inc., NY p. 623.

Pettit, N.B., Willatzen, M., Ploug-Sorensen, L., 1998, A general dynamic simulation model for evaporators and condensers in refrigeration. Part II: simulation and control of an evaporator, *Int. J. Ref.*, vol. 21, no. 5: p 404-414.

Rice, C.K., 1987, The Effect of Void Fraction Correlation and Heat Flux Assumption on Refrigerant Charge Inventory Predictions, *ASHRAE Trans.*, Vol. 93, Part 1: p. 341-367.

Thome, J.R., 2004, Void Fractions in Two Phase Flows, *Engineering Data book III,* Wolverine Tube Inc. http://www.wlv.com/products/databook/db3/DataBookIII.pdf , P.17.1-17.33.

Willatzen, M., Pettit, N. B., Ploug-Sørensen, L., 1998, A general dynamic simulation model for evaporators and condensers in refrigeration.next term Part I: moving-boundary formulation of two-phase flows with heat exchange, *Int. J. Ref.*, vol. 21, no. 5: p. 398-403.

WOJTAN, L, 2004, *Experimental and Analytical Investigation of Void Fraction and Heat Transfer During Evaporation in Horizontal Tubes*, Thèse No. 2978, ÉPFL, Lausanne, p. 126-132.

Wojtan, L., Ursenbacher, T., Thome, J. R., 2004, Interfacial measurements in stratified types of flow. Part II: Measurements for R-22 and R-410A, *Int. J. Multiphase Flow*, vol. 30, no.2 , pp. 125–137.